IOP Conf. Series: Materials Science and Engineering **152** (2016) 012057 doi:10.1088/1757-899X/152/1/012057

Three dimensional numerical investigations on the heat transfer enhancement in a triangular facing step channels using nanofluid

K A Mohammed[1*], **A R Abu Talib**[1,3], **N Abdul Aziz**[4] **and K A Ahmed**[1]

[1]Department of Aerospace Engineering, Universiti Putra Malaysia, Malaysia
[2]Department of Mechanical Engineering, College of Engineering, Universiti of Anbar, Anbar, Iraq
[3]Aerospace Manufacturing Research Centre, Universiti Putra Malaysia, Malaysia
[4]Department of Mechanical and Manufacturing Engineering, Universiti Putra Malaysia, Malaysia

*kafelazeez@yahoo.com

Abstract. In this paper, laminar flow for the distilled and SiO_2–water nanofluid flow and heat transfer were numerically investigated in three-dimensional triangular facing-step channel. The nanoparticle volume fraction and Reynolds number considered are in the range of 0–1% and 100–1500, respectively. Numerical solutions are obtained by using finite difference method to solve the governing equations. The effects of the volume fraction of nanoparticle, triangular facing-step channel amplitude height, wavelength and Reynolds number on local skin-friction coefficient, average Nusselt number and enhancement of heat transfer are presented and discussed. The results show that the Nusselt number and friction coefficient increases as the amplitude height of triangle channel increases. As the nanoparticle volume fraction increases, the Nusselt number is also found to be significantly increased, accompanied by only a slight increase in the friction coefficient. In addition, it is found that the heat transfer enhancement mainly depends on the amplitude height of the triangle wall, nanoparticle volume fraction and Reynolds number rather than the wavelength.

1. Introduction

Heat transfer improvement in the heat exchanger is essential in developing a compact one that has high thermal efficiency, light weight, small size and low manufacturing cost. It is known that deployment of corrugations walls can potentially lead to a better performance in heat transfer enhancement due to the mixing of the fluid by the corrugations surfaces. Investigation on the method for improvement of heat transfer in these devices has become necessary. In recent years, it is revealed that thermal conductivity of conventional heat transfer fluids such as oil, water, and ethylene glycol can be improved by adding nanoparticles. Aung [1] performed experimental work of two-dimensional (2D) laminar flow through a downstream facing-step. It was observed that a small fluctuation occurred at low values of Reynolds number (*Re*). The observed fluctuation was the onset of transition to the separated boundary layers. In addition, there was also a tendency towards a secondary separation at the upper wall due to velocity inflection profiles with high values of *Re*. Kherbeet *et al.* [2] reported their experimental heat transfer results of laminar flow of air passing through a facing-step channel with backward under constant wall

temperature. It was concluded that the heat transfer under laminar flow enhances in the direction of stream wise as compared to smooth channel and the optimum heat transfer is at the re-attachment point downstream. The velocity of separated airflow under laminar three-dimensional (3D) with a facing-step has been measured by Armaly *et al.* [3]. It was found that it has no recirculation flow region near the wall for low *Re*. On the other hand, a region of small recirculation flow appears at the upper corner of the sidewall for high *Re*. Nie and Armaly [4] measured the velocity near walls for 3D backward facing step flow. A comparison of the 2D at the downstream wall has been conducted for 3D at the channel center. Results of 3D were significantly lower for transition flow regime but slightly lower at regimes of turbulent and laminar flow. Hattori and Nagano [5] have studied boundary layer turbulent flow through a forward facing step. The separation regions have occurred on the step and in front of the forward facing step flow.

Many experimental studies of convective heat transfer of conventional fluid in corrugated channels at laminar flow condition have been carried out in the past [6, 7, 8, 9]. Rushet *et al.*[10] experimentally performed the study on the heat transfer and flow characteristics under sinusoidal wavy laminar flows through a channel. Water tunnel was used to study the flow field using visualization methods while wind tunnel has been used to conduct heat transfer experiments in the range of *Re* from 100 to 1000. It was observed that the geometry of the channel and *Re* have directly affected the location of the mixing onset. Heat transfer has significantly increased with onset of macroscopic mixing. The performance of the corrugated channel of 5 mm height spacing is better than that of the 10 mm height spacing. The studies on convective heat transfer through corrugated channels under turbulent flow conditions have been carried out by a number of researchers [11, 12, 13]. Oyakawa *et al.* [14] experimentally studied the influence of the channel height on the heat transfer improvement and pressure drop in a sinusoidal-wavy channel over the range of *Re* of 4000-200000. The wavelength and amplitude of wavy channel were 80 mm and 20 mm, respectively. Their results showed that the optimal performance of the wavy channel could be achieved when the ratio of wavelength to channel height was two. Additionally, the separation point of the flow was observed to be highly dependent on the channel height, while the reattachment point of the flow was independent of it. The flow characteristics and heat transfer of air flow in the corrugated channels under the conditions of constant surface temperature and *Re* ranging from 3220 to 9420 were studied experimentally by Elshafei *et al.* [15, 16]. The results indicated the influence of channel spacing variations on the heat transfer and the friction factor was dependent than the phase shift variation especially at high *Re*.

Nanofluid is metallic or non-metallic nanoparticles with a size of less than 100 nm dispersing in the liquids. A novel heat transfer fluid, prepared by suspending nanopowders in conventional heat transfer fluid to obtain higher thermal conductivity, is called as nanofluid [17]. Many attempts were conducted to suspend metal particles in conventional fluid as reported by Maxwel [18] and others but the main challenge was the large size of particles and weight. Nanofluids, on the other hand, have small sized nanoparticles with less sedimentation of particles suspension.

It has been acknowledged that efficiency of heat exchanger is still subject to further investigation. Therefore, this study considers new configurations that have not been investigated before with the aim of getting a better enhancement in heat exchanger. Furthermore, the study involves establishing the effects of variation in geometrical parameters such as amplitude height, wave length, Reynolds number and nanofluid on the Nusselt number, friction factor and pressure drop. Overall, the objectives are to enhance heat transfer using corrugated surface in back ward facing step model, investigate the effect of pressure drop and friction factor of flow region in corrugated facing step channel, and assess the effect of nanofluids with corrugated facing step channel.

2. Mathematical model

2.1. Physical domain definition

The geometry of the shape under investigation in the present problem is shown in Figure 1. It consists of a lower triangular corrugated plate with wavelength, L_w and amplitude height, a. The triangular wall

is isothermally heated to 24000 W/m^2. The triangular wall's total length is 20 cm, i.e. there are 2, 4, 5, and 10 cm waves along the triangular wall. For creating appropriate boundary conditions for both inlet and outlet of the triangular wall, two smooth adiabatic sections are considered: one is before the triangular wall section and the other is after it. The length of each smooth section is 70 cm and 20 cm, respectively, and the height of step is 1 cm. For this study, the following geometric dimensionless parameters are applied: triangular wavelength, L_w of 0, 2, 4, 5 and 10 cm, and triangular amplitude height, a of 0, 0.1, 0.2,0.3and 0.4 cm.

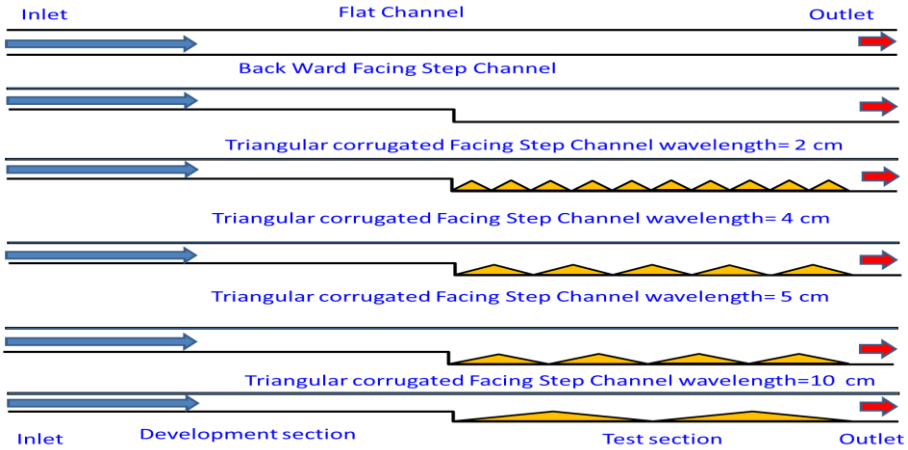

Figure 1. Schematic of the computational domain of flat channel, backward facing-step, triangular with wavelengths of 2, 4, 5 and 10 cm

2.2. Governing equations and problem assumptions in present study

The nanofluid is taken as Newtonian fluid and the flow is considered to be laminar, incompressible, steady and three-dimensional. Moreover, it is presumed that the mixture of solid particles and water enters the channel at similar temperature and velocity. Based on the assumptions, the non dimensional governing stream function, energy and vorticity transport equations for the mixture of nanoparticles and liquid are modelled and presented as (ANSYS Fluent, 14.5).

Continuity equation:
$$\nabla \cdot (\rho \vec{V}) = 0 \tag{1}$$

Momentum equation:
$$\nabla \cdot (\vec{V}\vec{V}) = -\frac{1}{\rho}\nabla p + v\nabla^2 \vec{V} \tag{2}$$

Energy equation:
$$\nabla \cdot (\vec{V}T) = \frac{1}{\rho_{\mathrm{nf}} c_{p_{\mathrm{nf}}}} k_{\mathrm{nf}} \nabla^2 T \tag{3}$$

where ρ is the density (kg/m^3), V is the velocity (m/s), p is the pressure (Pa), v is dynamic viscosity (kg/m.s), c_p is specific heat capacity (J/kg.K), k is thermal conductivity (W/m.K), T is temperature (K) and *nf* is nanofluid.

2.3. Thermophysical properties of nanofluids

These properties are calculated using the following equations. For effective thermal conductivity [19]:

$$k_{eff=} k_{static} + k_{Brownian} \tag{4}$$

$$k_{static} = k_{bf}\left[\frac{\left(k_{np}+2k_{bf}\right)-2\phi\left(k_{bf}+2k_{np}\right)}{\left(k_{np}+2k_{bf}\right)+\phi\left(k_{bf}+2k_{np}\right)}\right] \tag{5}$$

where k_{bf} and k_{np} are the base fluid and the thermal conductivity of the nanoparticle, respectively. The Brownian motion thermal conductivity is presented by Vajjha and Das [20] as:

$$k_{\text{Brownian}} = 5\times10^{4}\emptyset\beta\rho_{\text{bf}}C_{\text{p,bf}}\sqrt{\frac{KT}{2\rho_{\text{np}}R_{\text{np}}}}f(T,\emptyset) \tag{6}$$

where K is the Boltzmann constant, T is the fluid temperature and T_0 is the reference temperature. The term of $f(T,\emptyset)$ is a function of the particle volume fraction and temperature. The correlation of β is a function of the liquid volume that departures with a particle material, expressed in Table 1 as given by Vajjha and Das [21].The effective dynamic viscosity is given by Corcione [22]:

$$\frac{\mu_{eff}}{\mu_{bf}} = \frac{1}{1-34.8\left(\frac{d_{np}}{d_{bf}}\right)^{-0.3}\phi^{1.03}} \tag{7}$$

where $d_{bf} = \left[6M/N\,\pi\rho_{bf}\right]^{1/3}$ μ_{eff} and μ_{bf} are the effective dynamic viscosity of nanofluid and base fluid respectively, d_{np} is the nanoparticle diameter, d_{bf} and ϕ are the base fluid equivalent diameter and the nanoparticle volume fraction, respectively. M is the base fluid molecular weight.

Table 1. The value of β particles with its boundary conditions [21]

Type of particles	β	Concentration	Temperature
SiO_2	$1.9526(100\phi)^{-1.4594}$	$1\% \le \phi \le 10\%$	298 K ≤ T ≤ 363 K

The effective density is given as [22]:

$$\rho_{eff} = \left(1-\phi\right)\rho_{bf} + \phi\rho_{s} \tag{8}$$

where ρ_{bf} and ρ_{eff} are the base fluid and nanofluid densities, respectively, and ρ_s is the density of the nanoparticle. The effective nanofluid's specific heat at constant pressure, $(C_p)_{eff}$ is calculated using Equation 9 [22].

$$\left(Cp\right)_{eff} = \frac{\left(1-\phi\right)\left(\rho Cp\right)_{bf} + \phi\left(\rho Cp\right)_{s}}{\left(1-\phi\right)\rho_{bf} + \phi\rho_{s}} \tag{9}$$

where Cp_s is the heat capacity of the solid particles and Cp_{bf} is the heat capacity of the base fluid. Following [23], *Nu*, *Re* and friction factor are dimensionless parameters that can be calculated as follows.

$$Nu = \frac{hD_h}{k} \tag{10}$$

where h and k are the average heat transfer coefficient of fluid and thermal conductivity, respectively. The Reynolds Number *Re* is expressed as:

$$Re = \frac{\rho u_m D_h}{\mu} \tag{11}$$

where ρ, u_m and μ are density, mean fluid velocity over the cross-section of fluid and dynamic-viscosity, respectively. Meanwhile, the hydraulic diameter (D_h) is defined as in Equation 12.

$$D_h = \frac{4A}{P} \tag{12}$$

where P is the wetted perimeter and A is the area of the cross-section. The friction factor for fully developed flow is expressed as in Equation 13.

$$f = \frac{2\,\Delta p\,D_h}{L\,\rho\,u_m^2} \tag{13}$$

For example, Table 2 lists out the thermophysical properties of distilled water based fluids and SiO_2 nanoparticles [22].

Table 2. Thermophysical properties of distilled water based fluids and SiO_2 nanoparticles at T = 300 K

Thermophysical Properties	SiO_2	Water
ρ (kg/m^3)	2220	996.5
c_p (J/kg·K)	745	4181
k (W/m·K)	1.4	0.613
μ (Ns/m^2)	-	1 x 10^{-3}
β (1/K)	5.5 x 10^{-6}	2.75 x 10^{-4}

3. Numerical analysis

Cartesian coordinate system (x,y) of the non-dimensional form of stream function, vorticity transport and energy equations for the liquid–solid mixture are transformed into non-orthogonal curvilinear coordinate system (f,g). The governing equations with appropriate boundary conditions are discretized using the finite volume method. For the current study, the Poisson equation is solved to develop the computational mesh. The energy equations and vorticity transport are solved using the simple explicit method based on the time marching technique whereas the stream function equation is solved using relaxation method [24, 25]. As the iteration started, the stream function is calculated, and the energy and vorticity transport equations are solved to determine the temperature and vorticity for all nodes in computational domain. The iteration is continued until the sum of absolute residual for all parameters in computational domain is less than 10^{-5}. The constant time step used for all calculations is 10^{-3}.

4. Grid independence test and validation of numerical methods

In order to assess the grid independent result for water at Re=100, expansion ratio of 2, and heat flux of 24000 W/m^2 for triangular corrugated facing step. Five different sizes of grid are tested to check the effect of the grid density on the computational results as shown in Table 3. The results show that the grid size of 3000000 ensures grid-independent test and it is consequently employed during the course of this study.

Table 3. Grid independence test

Grid number	Average Nusselt Number	Relative Error*	% Relative Error
46875	8. 1311889	----------	----------
375000	8. 1460963	1.83*10-3	0.18 %
1736110	8. 1489158	3.46*10-4	0.034 %
3000000	8. 1496036	8.44*10-5	0.008 %
5859375	8. 1501611	6.84*10-5	0.0068 %

*Relative error = $(Nu_{new} - Nu_{previous})/Nu_{new}$

The validation studies are carried out for laminar distilled water and 5% copper-water nanofluid flow in the straight channel. The numerical results are then compared with that of Santra *et al.* [26], which include the inlet temperature of 293K, upper and lower wall preserve at uniform wall temperature condition, height of channel (0.01 mm), channel length and the diameter of nanoparticles (100 nm). The result shows a good agreement as shown in Figure 3.

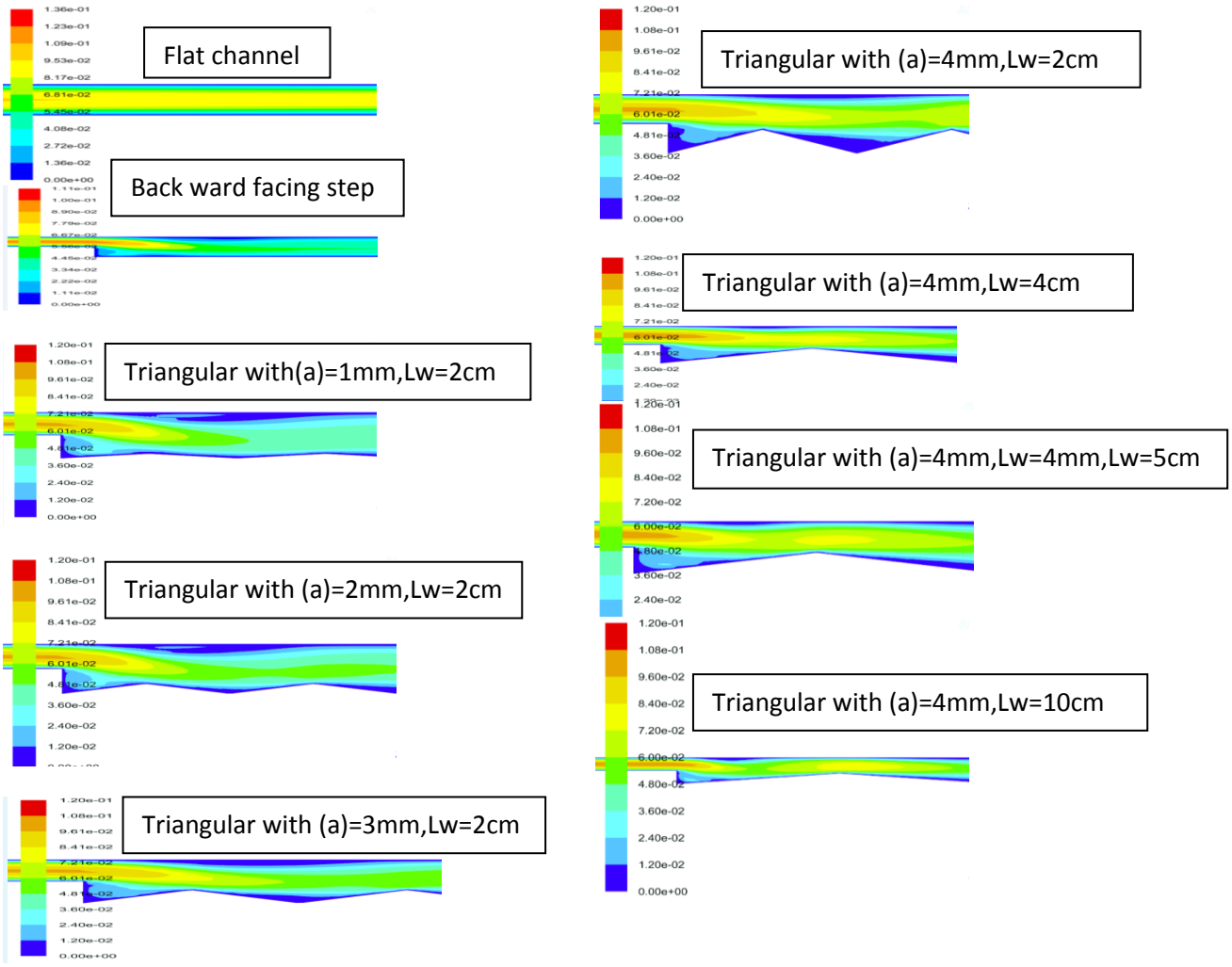

Figure 2. Streamlines (top) and isotherms (bottom) for nine different geometries at *Re* = 750, without amplitude height (*a*), and wave length (L_w)

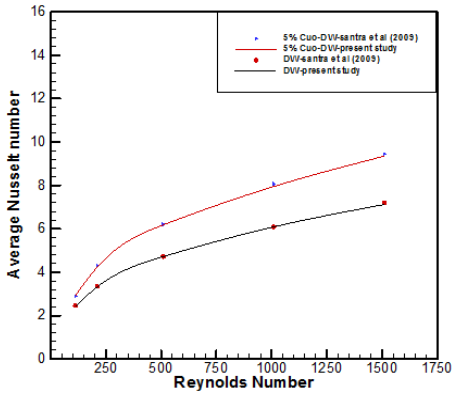

Figure 3: Comparison of the average *Nu* for present study with previous numerical study in [26]

Figure 4 shows the comparison between numerical results of this study and experimental data of Mohammed *et al.* [27]. The average Nusselt number for 1% SiO_2-water nanofluid at L_w = 20 mm and d_p = 30 nm triangular corrugated channel with amplitude length of 1.5 mm is shown to be in a good agreement between the two data with only 3% of error percentage.

5. Results and discussion

Figure 5 shows the effect of channel shape, triangular amplitude height and *Re* on *Nu* in the laminar flow region. It is found that the highest *Nu* is obtained by the triangular with amplitude height of 4mm, followed by triangular with amplitude heights of 3, 2, 1, 0 mm and the lowest *Nu* optioned by flat channel. It can be observed the enhancement of thermal conductivity due to the area increase as the amplitude height for triangular shape rises. Moreover, the effect of different *Re* in the range of 100 to 1500 shows that the Nusselt number increases as Reynolds number increases. Figure 6 shows the effect of the geometry parameters and *Re* on the pressure drop in the laminar flow region. It is clearly shown that by increasing *Re* from 100 to 1500, the pressure dropped significantly from the inlet of the duct to the outlet. It is also found that the lowest pressure drop corresponds to the flat channel while the highest pressure drop is obtained by the triangular having amplitude height of 4 mm, followed by triangular having amplitude heights of 3, 2, 1 and 0 mm. Figure 7 shows the effect of amplitude height and Reynolds number on the friction factor along the triangle corrugated facing step channel. It can be seen that the friction decreases with the increase in Reynolds number. On the other hand, the friction factor increases with increasing amplitude height.

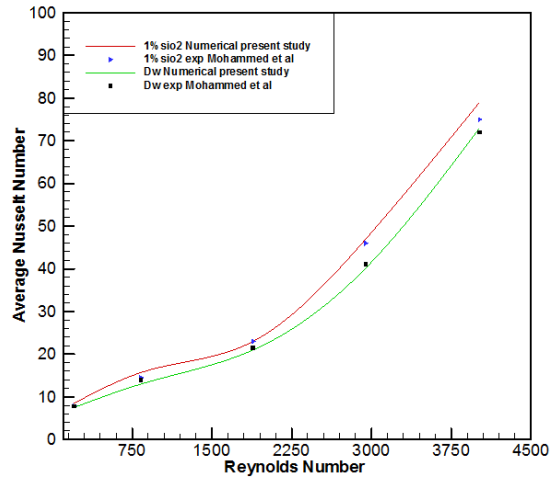

Figure 4. Comparison between numerical present study results and measured data in [27]

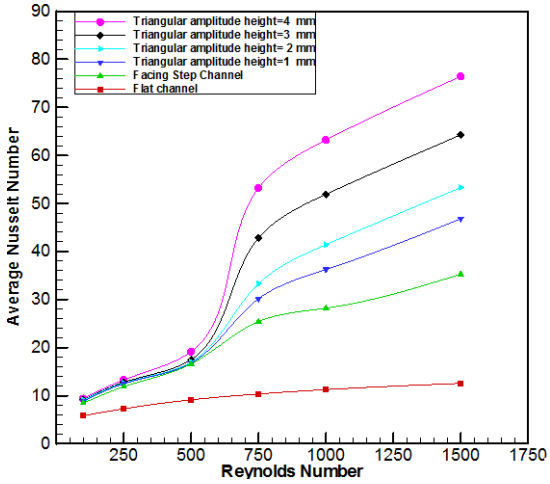

Figure 5. Effect of channel shape and triangular amplitude height to *Nu* in laminar flow region

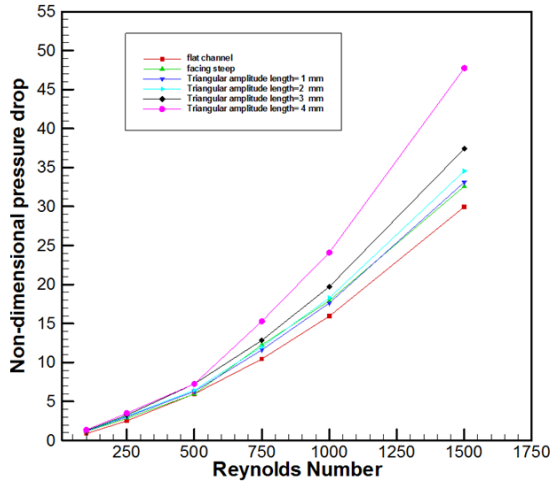

Figure 6. Effect of channel shape and triangular amplitude length to pressure drop in the laminar flow region

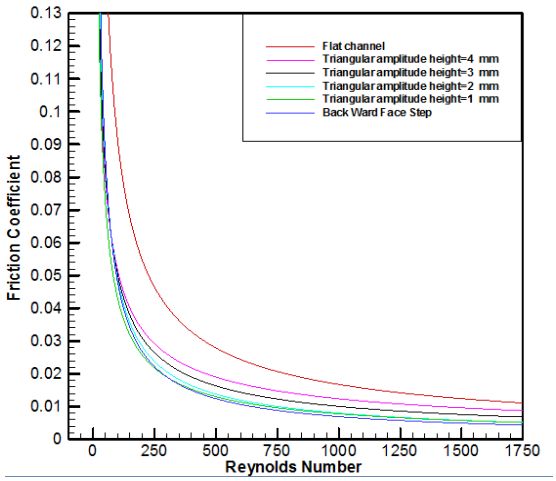

Figure 7. Effect of channel shape and triangular amplitude height to friction factor

Figure 8 shows the effects of wavelength to the Nusselt number for four different wavelengths, L_w from 0, 2,4,5 and 10 cm. The result shows that the wavelength of 2 cm gives a better enhancement and *Nu* decreases with increasing wavelength. Meanwhile, Figure 9 shows the effect of adding 1% SiO_2 nanofluid to the base fluid for three types of channels: flat, backward and triangular facing-step. It can be seen that *Nu* increases with addition of nanoparticle to the base fluid and the triangular channel with amplitude height of 4 mm gives better enhancement.

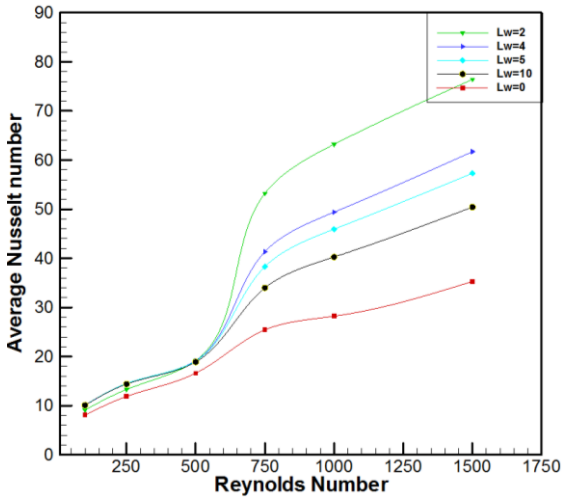

Figure 8. The effect of different wavelength, L_w with *Re* to *Nu* in laminar flow region

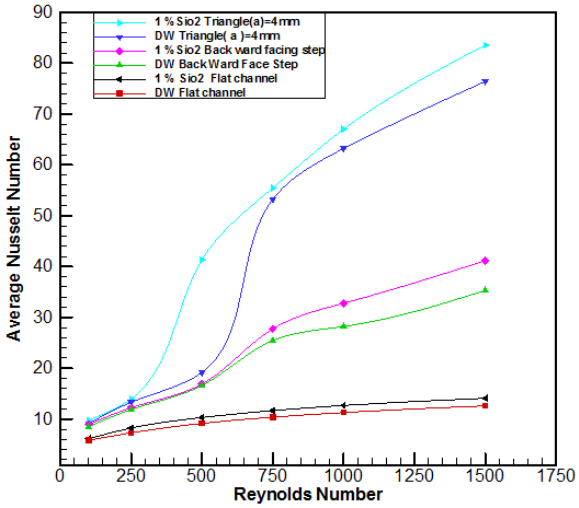

Figure 9. Effect of added 1% SiO_2 nanofluid to *Nu* for different shapes of channel, triangular amplitude length 4 mm in laminar flow region

6. Conclusion

In the current study, three dimensional in three types of channels are examined using finite difference method for a range of Reynolds number, *Re* between 100 to 1500 and nanoparticle volume fraction range of 0–1%. The effect of Reynolds number *Re*, nanoparticle volume fraction, height of amplitude and wavelength of the triangular wall on the average *Nu*, local skin-friction coefficient, heat transfer enhancement and pressure drop are presented and analyzed. The results show that the skin-friction coefficient for the base fluid increases with the increase in the amplitude height of triangular wall. In addition, it is found that the improvement in heat transfer essentially depends on amplitude height, *Re* and nanoparticle volume fraction of the triangular wall rather than the wavelength. Finally, the results of this study ensures that using nanofluid instead of distilled water in the triangular facing step channel can lead to further improvement in the thermal performance of heat exchangers.

References

[1] Aung W 1983 *Journal of Heat Transfer* **105** 823-9
[2] Kherbeet A S, Mohammed H and Salman B 2012 *International Journal of Heat and Mass Transfer* **55** 5870-81
[3] Li A and Armaly B F 2000 *Proceedings of the ASMEIMECE conference*
[4] Armaly B F, Li A and Nie J 2003 *International Journal of Heat and Mass Transfer* **46** 3573-82
[5] Hattori H and Nagano Y 2010 *International Journal of Heat and Fluid Flow* **31** 284-94
[6] Sparrow E and Comb J 1983 *International Journal of Heat and Mass Transfer* **26** 993-1005
[7] Sawyers D R, Sen M and Chang H-C 1998 *International Journal of Heat and Mass Transfer* **41** 3559-73
[8] Pehlivan H, Taymaz I and İslamoğlu Y 2013 *International Communications in Heat and Mass Transfer* **46** 106-11
[9] Patel V, Chon J T and Yoon J 1991 *Journal of Fluids Engineering* **113** 579-86

[10] Rush T, Newell T and Jacobi A 1999 *International Journal of Heat and Mass Transfer* **42** 1541-53
[11] Islamoglu Y and Parmaksizoglu C 2003 *Applied Thermal Engineering* **23** 979-87
[12] Parsazadeh M, Mohammed H and Fathinia F 2013 *International Communications in Heat and Mass Transfer* **46** 97-105
[13] Namburu P K, Das D K, Tanguturi K M and Vajjha R S 2009 *International Journal of Thermal Sciences* **48** 290-302
[14] Oyakawa K, Teruya I, Senaha I, Yaga M and Mabuchi I 1996 *Trans Jpn Soc Mech Eng Ser B* **62** 1104-10
[15] Elshafei E, Awad M, El-Negiry E and Ali A 2010 *Energy* **35** 101-10
[16] Elshafei E, Awad M, El-Negiry E and Ali A 2008 *Second International Conference on Thermal Issues in Emerging Technologies*
[17] Nguyen C, Desgranges F, Roy G, Galanis N, Maré T, Boucher S and Mintsa H A 2007 *International Journal of Heat and Fluid Flow* **28** 1492-1506
[18] Yu W and Choi S U S 2003 *Journal of Nanoparticle Research* **5** 167-71
[19] Ghasemi B and Aminossadati S 2009 *Numerical Heat Transfer, Part A: Applications* **55** 807-23
[20] Vajjha R S and Das D K 2009 *International Journal of Heat and Mass Transfer* **52** 4675-82
[21] Vajjha R S, Das D K and Kulkarni D P 2010 *International Journal of Heat and Mass Transfer* **53** 4607-18
[22] Corcione M 2010 *International Journal of Thermal Sciences* **49** 1536-46
[23] Eiamsa-Ard S and Promvonge P 2009 *International Communications in Heat and Mass Transfer* **36** 705-11
[24] Anderson J D 1995 *Computational Fluid Dynamic: The Basics with Applications* (New York: McGraw-Hill)
[25] Anderson J D and Wendt J 1995 *Computational Fluid Dynamics* (Berlin: Springer)
[26] Santra A K, Sen S and Chakraborty N 2009 *International Journal of Thermal Sciences* **48** 391-400
[27] Mohammed A, Yusoff M, Ng K and Shuaib N 2015 *Case Studies in Thermal Engineering* **6** 77-92